Nonlinear Dynamics (2006) 45: 385–397
DOI: 10.1007/s11071-005-9014-8

Railway Train-Track Dynamics for Wheelflats with Improved Contact Models

L. BAEZA* , A. RODA, J. CARBALLEIRA, and E. GINER
Dpto. Ingeniería Mecánica y Materiales,Universidad Politécnica de Valencia. Camino de Vera, 14. E-46022 Valencia, Spain; (e-mail: Lbaeza@mcm.upv.es; fax: +34963877629)

(Received: 28 June 2005; accepted: 7 November 2005)

Abstract. A variety of methods have been proposed to calculate the dynamic response caused by a railway vehicle affected by a wheelflat. Most of the sophisticated procedures evaluate the elastic properties of the wheel-rail contact by means of the Hertz model. However, the hypotheses that must be satisfied in order to apply the Hertzian contact model are not fulfilled when the wheel-rail contact occurs in the area of wheel affected by the flat. This gives rise to deviations in the results of the dynamic model compared to the real situation. With the objective of analysing the influence of the elastic wheel-rail contact model, a procedure was developed to determine the dynamic response caused by a geometric irregularity (in rail or wheel) by means of Hertzian and non-Hertzian contact models. Results of the wheelflat impact simulations given by both types of contact model have been compared in this work.

Key words: train-track dynamics, wheelflat, Hertzian contact model

1. Introduction

There have been a considerable number of defects in wheels whose results and (occasionally) causes are related to a dynamically coupled process between the track and the railway vehicle. This type of defects correspond to deviations in the geometry of the wheel tread from its original circular shape, also known as Out-of-Round (OOR). OOR is catalogued by the UIC in [1] and has been extensively studied by Nielsen and Johansson in [2, 3]. In [3] flats are given as the cause of the increased force transmitted from wheel to rail in the OOR wheels analyzed in the field studies. The consequences of crack growth in rails caused by the impact of a wheelflat are analyzed in [4].

Various models for calculating the dynamic coupling between railway vehicle and track allow to obtain the force response caused by a wheelflat. There are a number of initial hypotheses that are common to most of the proposed methodologies. Thus, it is frequent to consider only the unsprung masses of the vehicle, since the primary suspension filters the high frequency vibration originated in the wheel-rail contact; only the vertical dynamics are considered since there generally exists a weak coupling of the lateral and vertical dynamics; symmetry is established with respect to the track axis, since the flats appear symmetrically on both wheels.

Nevertheless, there can be found highly sophisticated models such as [5], which realistically considers the track-vehicle system in all its complexity as a three dimensional problem. Other models, such as [6], establish a set of basic hypotheses that give industrially useful results with a low computational cost. However, practically all the models determine the wheel-rail contact forces by means of the Hertz formula, which relates the normal transmitted force F_c with the approach between bodies δ according to the equation

$$F_c = K_H \delta^{1.5} \tag{1}$$

where K_H is a constant that depends on the mechanical properties of the materials and on the geometry of non-deformed bodies in contact. More sophisticated non-Hertzian contact models have been used to calculate rail corrugation in [7] and vehicle dynamics in the low-frequency range in [8].

The initial fundamental hypotheses of the Hertzian contact model are given in Reference [9]. They include the geometric requirement by which the non-deformed surfaces of the bodies in contact should be elliptic paraboloids. This requirement is not satisfied when the rail-wheel contact coincides with, or is near to, the flat. This makes it necessary to evaluate the limitations of using the Hertzian contact model by means of Equation (1).

The main objective of this paper is to analyze the effects of improvements in the wheel-rail contact model on the response produced by a wheelflat. The basic idea is to evaluate the tendency to deviate from the real situation when Hertzian contact models are used to simulate the dynamics produced by a flat. With this objective, we will compare the theoretical results derived from a Hertzian contact model with those from a non-Hertzian model, in which the elastic contact characteristics in the area around the flat are determined with greater precision. The non-Hertzian model chosen was proposed by Kalker in [10]. In Section 4 a description of the characteristics of this model and the reasons for which it was selected is given. The simulation model had previously been presented in Reference [11]. Its basic characteristics are described in Section 2.

2. Dynamic Simulation Model

The model presented in [11] allows to calculate the coupled dynamics between the vehicle and the track. This is a hybrid model that combines physical and modal coordinates, in which the response is obtained in time domain by means of numerical integration. The vertical dynamics of the system are considered, as well as the possibility of the existence of asymmetric behaviour with respect to the axis of the track.

The proposed model considers the global system formed by three types of substructures: rails, sleepers and the vehicle. Each of these elements by itself has characteristics that could be considered as linear. The non-linear characteristics are located in the elements that connect the substructures to each other: the wheel-rail contact, ballast and railpads.

Rails and sleepers are continuous elements that are considered through a modal approach. Their modal properties can be calculated from a Timoshenko beam model, examining each element individually. Thus, if ϕ_m^i is the m-th vibration mode normalized with regard to the mass of the substructure i (rail or sleeper), the vertical displacement of a point located through the longitudinal coordinate x at an instant of time t is

$$v^i(x,t) = \sum_{m}^{N_i} \phi_m^i(x)\, q_m^i(t) \tag{2}$$

where $q_m^i(t)$ constitute a set of modal coordinates defined for each substructure. It should be noted that in the previous equation a modal truncation was performed when a finite number of N_i vibration modes was considered for each substructure.

The foregoing coordinates are augmented to a greater set from which it is possible to define a phase space [12]. The set of phase coordinates is defined by $q_m^i(t)$ and $p_m^i(t)$, for each substructure i (rail

or sleeper), where m varies from 1 to the number of modes N_i. These coordinates define the modal movement equations through the following expressions

$$\begin{aligned} \dot{q}_m^i(t) &= -2\,\zeta_m^i\;\omega_m^i\;q_m^i(t) + p_m^i(t) \\ \dot{p}_m^i(t) &= -\left(\omega_m^i\right)^2\,q_m^i(t) + f_m^i(t) \end{aligned} \tag{3}$$

where ζ_m^i is the modal damping ratio, ω_m^i is the non-damped natural frequency and $f_m^i(t)$ is the modal force of mode m in the substructure i. $\dot{p}_m^i(t)$ is zero if the response associated to the mode is quasistatic, and consequently this variable could be used for estimating the dynamical influence of the mode m on the global system response.

The modal force $f_m^i(t)$ is calculated through modal transformation from the forces applied to each substructure. These are the forces transmitted through the wheel-rail contact and rail pads. The forces are calculated by means of the relative displacements and velocities of the points that they join. For example, in the specific case of the Hertzian model, Equation (1) will be used, while for more complex models a non-analytical relationship may be used, as is explained in Section 4.

Considering the vehicle as a multi-body system formed by axles and frames, the equations that determine its dynamics for small displacements can be expressed as the classic vibration equation (lumped mass and stiffness) given by

$$\mathbf{M}\,\ddot{\mathbf{w}} + \mathbf{D}\,\dot{\mathbf{w}} + \mathbf{K}\,\mathbf{w} = \mathbf{F}_{\mathbf{ext}} \tag{4}$$

where in $\mathbf{w}$ the singular point coordinates corresponding to the vehicle are considered, $\mathbf{M}$, $\mathbf{D}$ and $\mathbf{K}$ are, respectively, the matrices of mass, viscous damping and stiffness, and in $\mathbf{F}$ the forces external to the vehicle are stored (basically weight forces and forces involved in the wheel-rail contact).

The set of differential equations given for each sleeper and rail by (3) and for the vehicle by (4) is coupled by the formulae associated with the forces transmitted between substructures. The set of ODEs is integrated by a standard Runge-Kutta type numerical procedure carried out on a NAG$^{\text{TM}}$ library program. The advantage of the proposed method lies on its low computational cost, as only a small number of coordinates have to be considered, and on the simplicity with which complex models of wheel-rail contact, rail pads and ballast can be introduced.

3. Geometry of Wheel-Rail Contact

In the literature concerning the study of the impact effect of flats, two kinds of flat geometry are considered (see Figure 1): firstly, the fresh flat, or the newly formed flat in the instant that it appears as a result of wheel-locking due to brake action. The second is the rounded flat associated with the geometry into which the fresh flat rapidly degenerates by the wear on its vertices. The fresh flat is characterized by its length L_o and by its depth d, both parameters being related by means of the chord equation according to

$$L_o = \sqrt{8\,R\;d - 4\;d^2} \tag{5}$$

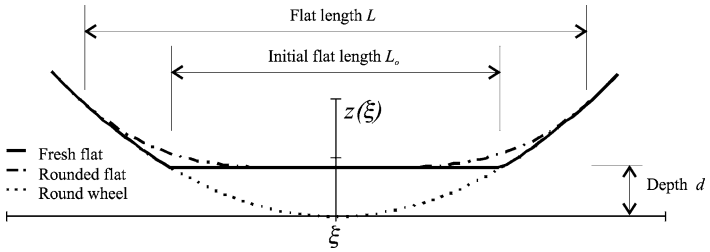

Figure 1. Geometry of fresh and rounded flats.

R being the wheel radius. The equation that defines the perimeter of the wheel containing the fresh flat is

$$z_F(\xi) = \begin{cases} R - \sqrt{R^2 - \xi^2} & |\xi| \geq L_o/2 \\ d & |\xi| < L_o/2 \end{cases} \tag{6}$$

where ξ is the coordinate according to the direction of the rail that defines the position of the point of the wheel under consideration.

The shape of the rounded flat in general is not sufficiently well-defined and ought to be made a subject of investigation. In the literature on this subject, a rounded flat is frequently given the same depth as the fresh but a greater length. The references often includes definitions of rounded flats by means of simple analytic functions [6]. A theoretical approximation to the rounded form of the flat can be made by means of the function

$$z_R(\xi) = \begin{cases} R - \sqrt{R^2 - \xi^2} & |\xi| \geq \frac{L}{2} \\ R - \sqrt{R^2 - \xi^2} + \dfrac{L^2}{4R\pi^2}\left(1 + \cos\dfrac{2\pi\xi}{L}\right) & |\xi| \leq \frac{L}{2} \end{cases} \tag{7}$$

where L is the length of the rounded flat. The minimum value of L that guarantees the convex form of the perimeter of the wheel by means of Equation (7) is $L = 4\sqrt{R\,d}$.

The methodology followed for analysing the geometric problem is the Improved Model developed by Tunna in [13]. The irregularity function is defined as the vertical displacement of the wheel from a reference position for bringing wheel and rail in contact. The reference position is chosen in such way that the irregularity function is zero if the wheel is perfectly rounded. The perimeter geometry allows the irregularity function to be calculated. Two examples of the irregularity function, deduced from the defect geometries considered in Equations (6) and (7), are shown in Figure 2. The irregularity function and the displacements in the wheel and the rail in the contact point are used to obtain the approach and the contact force (see Chapter 4).

In the model constructed for this study, the contact geometry must also be taken into account for the calculation of the elastic properties of rail-wheel contact. It is therefore necessary to make a spatial description of the contact geometry. With the objective of determining the elastic contact properties, the geometry of the rail profile was modeled in the form of a cylinder, and that of the wheel in the form of a conical surface. Thus, for a GV40 wheel profile on a UIC60 rail, the cylinder representing the rail has a radius of 300 mm, while the cone corresponding to the wheel has a slope of 1:40. The surface of the fresh flat on the wheel is a cylindrical surface, corresponding to the shape of the rail on which it was produced (see the sketch in Figure 3). The profiles of the wheel sections perpendicular to the wheelset

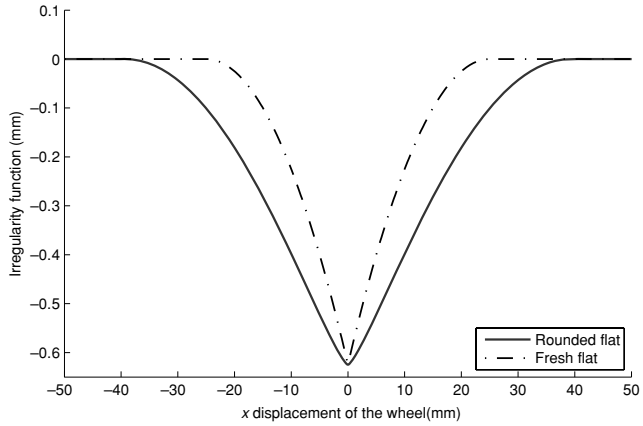

Figure 2. Irregularity functions calculated from Equations (6) and (7). The initial flat length L_o is equal to 50 mm in a wheel of 1000 mm diameter.

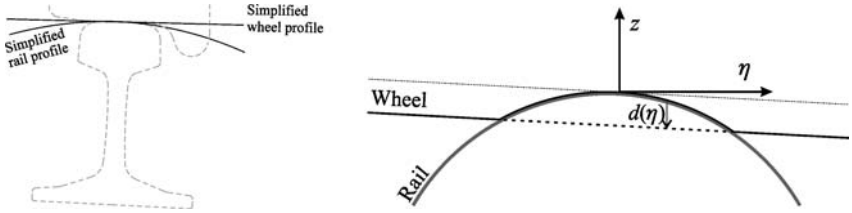

Figure 3. Simplified geometry of rail and wheel.

axle are similar to that shown in Figure 1. These profiles can be obtained through Equation (6). The d and L_o parameters that must be included in Equation (6) are functions of the section studied. There exists a distribution $d(\eta)$ as a function of the coordinate η, where η defines the lateral position with respect to the theoretical wheel rail-contact point. The $d(\eta)$ distribution is obtained from the wheel and rail geometry and the flat depth or $d(0)$. For each plane perpendicular to the wheelset axle defined by η could be obtained a wheel perimeter through Equations (6) and (7), and consequently the wheel tread geometry can be determined.

4. Elastic Model of Wheel-Rail Contact

The geometries of bodies in contact defined in Chapter 3 are characterized for having curvature radii much greater than the dimensions of the contact area and the length of the flat. The vertex of the fresh flat is an exception to this hypothesis. This is a single point at which the contact traction present are so high that it causes the material to yield so that the initial geometry rapidly becomes rounded. Nevertheless, taking into account the dimensions of the flat in relation to the wheel diameter, the vertex of the flat has a very obtuse angle, so that its singularity has very small effect on the contact stiffness. If this factor is neglected, it is possible to establish the non-conformal contact hypothesis in the elastic problem (according to the definition of non-conformal contact in [14]).

The proposed methodology for considering non-Hertzian models requires a table to be drawn up in which, for a set of combinations of transmitted force and different positions of flat with respect to the

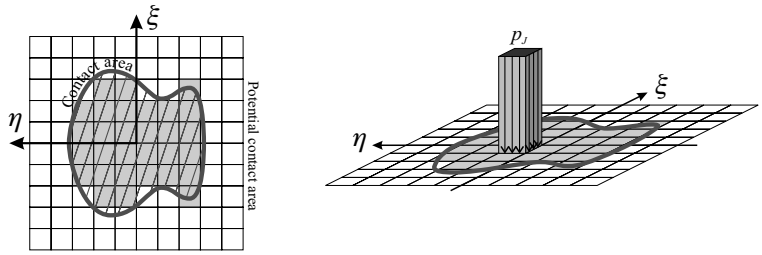

Figure 4. Definition of the potential contact area.

contact, the approach between bodies δ can be determined. The calculation of the contact problem is based on the method developed by Kalker for non-conformal non-Hertzian normal contact modeling. The complete description of this method may be found in reference [10], but the process can be summarized as follows.

The potential contact area (PCA) is arbitrarily defined in such way that it contains every point of the contact area. In order to keep the method simple, the PCA is rectangular. A discretization of the PCA is established in equal rectangular elements within which the magnitudes to be defined in each element are considered to be constant (see Figure 4). For the J-th element, these magnitudes are the displacement associated with the elastic deformations u_J, the normal traction p_J and the distance between the non-deformed surfaces of wheel and rail h_J.

Defining the elements that belong to the area of contact, the contact problem is solved by means of the following set of algebraic equations

$$\left.\begin{aligned} 0 &= \delta + h_J + \sum_I D_{JI}\, p_I \quad \text{if } J \in \text{Contact area} \\ 0 &= p_J \qquad\qquad\qquad\quad \text{if } J \notin \text{Contact area} \end{aligned}\right\} \tag{8a}$$

$$0 = F_c - S \sum_J p_J \tag{8b}$$

where S is the area of each element and A_{JI} corresponds to the displacement in element J when a unit load is applied in I. The coefficients A_{JI} can be calculated analytically, supposing that the bodies behave elastically as an infinite half-space. In this case, can be deduced from the expression that relates the displacement at a point (ξ, η) when a normal traction p is applied within a rectangle measuring $2a \times 2b$ centered on the origin. This displacement, according to the Young's modulus E and Poisson ratio ν, was calculated by Love in [15]

$$\begin{aligned} u(\xi,\eta) = \frac{p\,(1-\nu^2)}{\pi E} \Bigg[& (\xi+a)\,\log\left(\frac{(\eta+b)\sqrt{(\xi+a)+(\eta+b)}}{(\eta-b)\sqrt{(\xi+a)+(\eta-b)}}\right) \\ & +(\eta+b)\,\log\left(\frac{(\xi+a)\sqrt{(\xi+a)+(\eta+b)}}{(\xi-a)\sqrt{(\xi-a)+(\eta+b)}}\right) \\ & +(\xi-a)\,\log\left(\frac{(\eta-b)\sqrt{(\xi-a)+(\eta-b)}}{(\eta+b)\sqrt{(\xi-a)+(\eta+b)}}\right) \\ & +(\eta-b)\,\log\left(\frac{(\xi-a)\sqrt{(\xi-a)+(\eta-b)}}{(\xi+a)\sqrt{(\xi+a)+(\eta-b)}}\right)\Bigg] \end{aligned} \tag{9}$$

where log is the natural logarithm function.

5. Calculation of the Elastic Properties of Contact

The model presented in Chapter 4 provides a method for determining the elastic properties of contact and makes it possible to establish a more precise model than that given by Equation (1). The wheel and rail geometry determines the non-deformed distances between bodies h_J used in Equation (8a), and consequently the value of δ according to the normal force transmitted. Figure 5 shows the influence of the wheelflat geometry by showing the value of the approach δ calculated for a normal load of 100 kN. The result is obtained according to the position of the flat with respect to the wheel-rail contact, given by means of the longitudinal displacement x of the wheel (for $x = 0$ there is full contact of the flat with the rail). The calculation was performed for the geometries of a fresh flat, a rounded flat, and also for the intermediate geometry given by their mean. The graph also shows the approach calculated by the Hertzian model. The divergence of the non-Hertzian model with respect to the Hertz model will significantly affect the results presented in Chapter 6, corresponding to the dynamic simulation model.

The approach calculation for a given value of the normal force involves a high computational cost when solved simultaneously with the ODEs associated to the dynamics. For this reason, the proposed methodology requires (previous to the integration of the ODEs) a sufficiently refined table in which the value of δ is determined according to the normal force and the position of the flat with respect to the contact. Figure 6 shows the result of this calculation for a fresh flat and Figure 7 that of the corresponding rounded geometry. The PCA discretization was performed on a grid of 50×50 elements fitted to the contact area.

For each position of the flat with regard to the contact, the relationship between force and displacement can be fitted by a function type

$$F_c = K\,\delta^a \tag{10}$$

The K and a parameters are determined for a set of positions of the wheel in relation to the flat, calculated by least square fitting. Parameter a has the value of 1.5 for wheel positions that place the

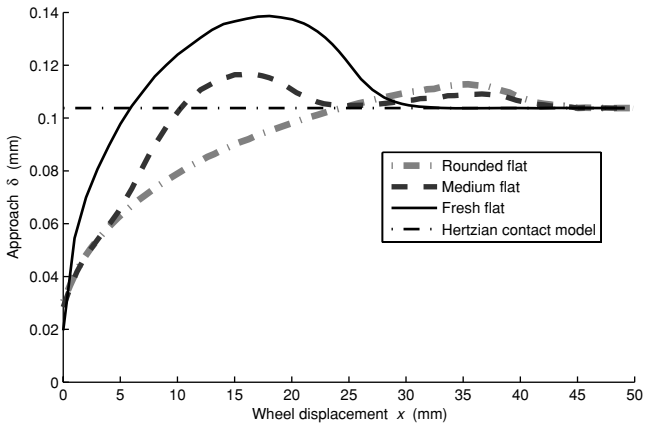

Figure 5. Results of the contact problem for a flat of initial length $L_o = 50$ mm (length of rounded flat $L = 70.7$ mm) on a wheel of 1000 mm diameter on an UIC60 rail. Calculated for a normal force of 100 kN and three different flat geometries.

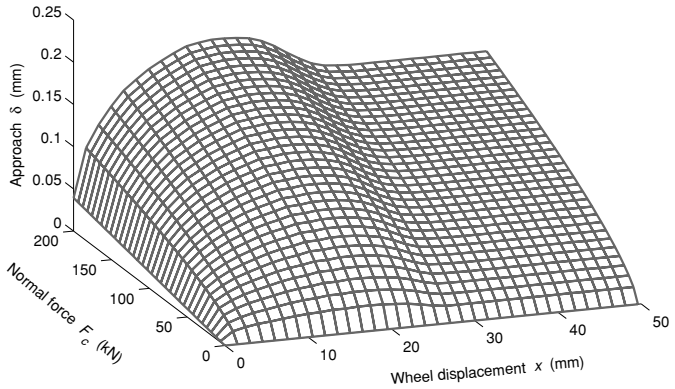

Figure 6. Result of the calculation of the contact problem for a fresh flat of $L_o = 50$ mm on a 1000 mm diameter wheel on a UIC60 rail.

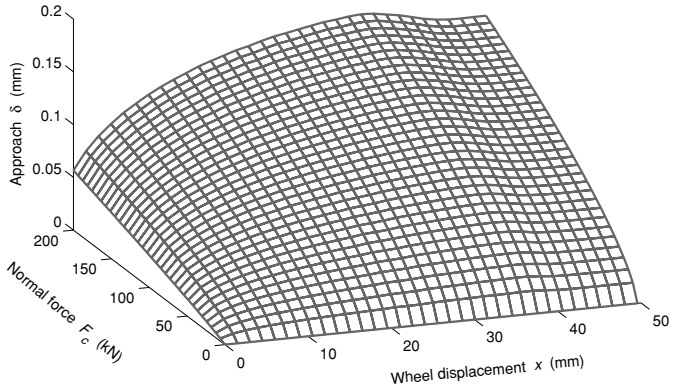

Figure 7. Result of the calculation of the contact problem for a rounded flat of $L_o = 50$ mm (length $L = 70.7$ mm) on a 1000 mm diameter wheel on a UIC60 rail.

flat out of contact, which coincides with the exact solution given by the Hertz model. When the flat is positioned on the rail, a tends to unity, especially for fresh flats. This is due to the fact that when contact occurs in the flat, the contact area has practically no dependence on the load ('complete contact' according to Hills and Nowell's definition in [14]).

6. Results of the Dynamic Simulation

The differences detected in the contact problem have a significant influence on the dynamic response of the system. This effect can be appreciated in Figure 8 in three calculations corresponding to a fresh flat, a rounded flat and an intermediate geometry, all calculated from the data obtained from a non-Hertzian contact model. The calculations were carried out for two practical cases (Cases A and B) whose parameters are given in Table 1. The parameters corresponding to these cases are based on those presented in [16, 17]. Case A corresponds to a track model with higher eigenvalues (the ballast is stiffer

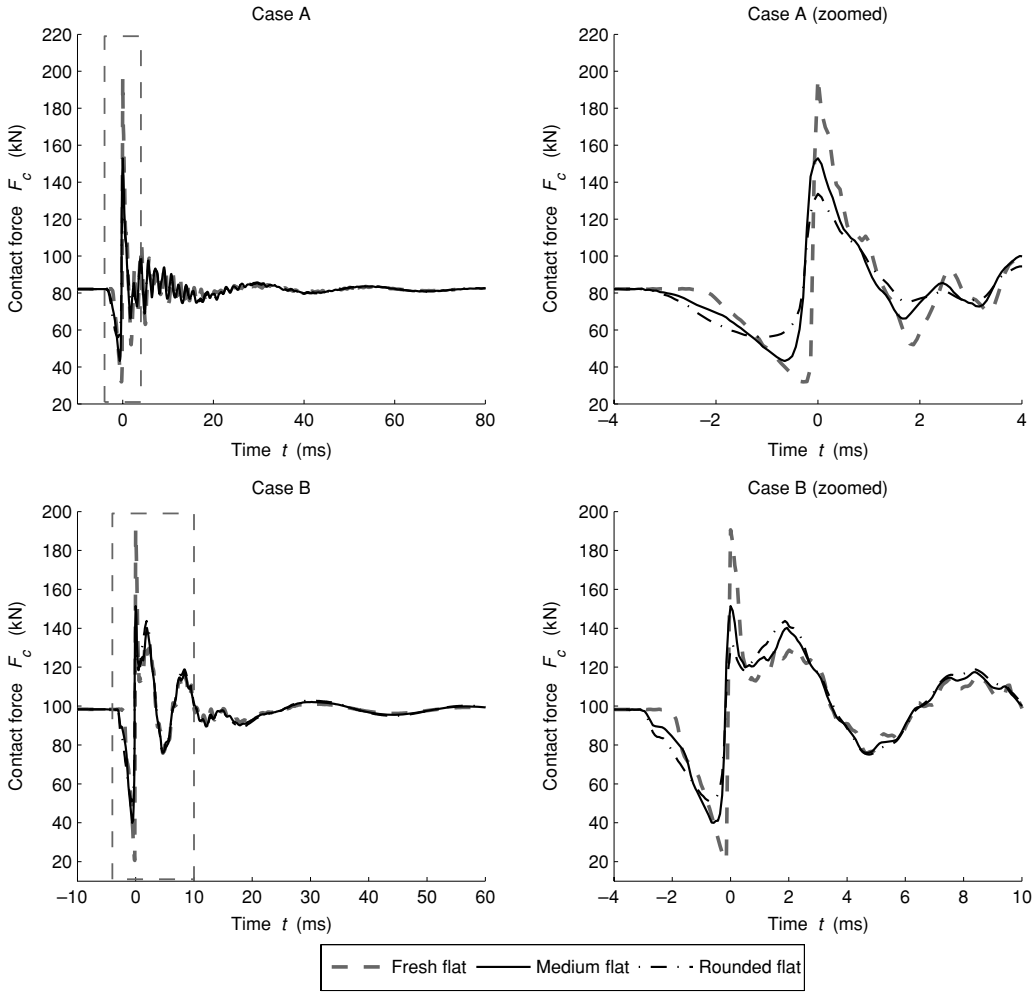

Figure 8. Contact force caused by a flat of initial length $L_o = 50$ mm on a wheel of 1000 mm diameter on an UIC60 rail for various flat geometries. Vehicle speed 50 km/h.

and the wooden sleepers are lighter) than those of case B (the ballast is softer and the concrete sleepers are heavier). With the aim of exciting all the modes of the rail, complete flat-rail contact occurs in a sleeper bay at a distance from the sleeper equal to $1/\sqrt{2}$ times the length of the sleeper bay. The flat length used in the calculations is $L_o = 50$ mm, the limit imposed by RENFE (the Spanish National Railways) for the repair of a wheel. The flat depth is 625 μm. In the calculations, the rounded flat has the same flat depth as the fresh flat.

The discrepancies between the simulation results for the different contact models can be seen in Figures 9 and 10. Figure 9 shows the peak force in the contact with the Hertzian and non-Hertzian model calculated for a range of speeds between 10 and 200 km/h. In Figure 10 the relative error ε committed by computing the peak force in the contact with the Hertzian model $F^H_{\max}$ was calculated. In calculating the relative error, the peak value deduced from the non-Hertzian model $F^{NH}_{\max}$ was taken as

Table 1. Parameters used in the model.

	CASE A	CASE B
Sleeper spacing	790 mm	650 mm
Sleeper length	2360 mm	2360 mm
Young's modulus of sleeper	10^9 N/m^2	20×10^9 N/m^2
Area of sleeper	15.73×10^{-3} m^2	15.73×10^{-3} m^2
Second moment of area of sleeper	11.8×10^{-6} m^4	11.8×10^{-6} m^4
Mass of sleeper	100 kg	250 kg
Sleeper foundation stiffness	26.78×10^6 (N/m)/m	25.84×10^6 (N/m)/m
Young's modulus of rail	207×10^9 N/m^2	210×10^9 N/m^2
Area of rail	7.17×10^{-3} m^2	7.69×10^{-3} m^2
Second moment of area of rail	23.5×10^{-6} m^4	30.5×10^{-6} m^4
Rail mass per unit length	56 kg/m	59.98 kg/m
Shear modulus of rail	81×10^9 N/m^2	81×10^9 N/m^2
Timoshenko shear coefficient of rail	0.34	0.34
Pad stiffness	200×10^6 N/m	80×10^6 N/m
Pad damping	21.8×10^3 N s/m	15×10^3 N s/m
Ballast damping	21.8×10^3 N s/m	31×10^3 N s/m
Total number of axles	4	4
Mass of axle	1000 kg	1600 kg
Mass of bogie frame	3000 kg	3000 kg
Mass of truck frame	56892 kg	67600 kg
Stiffness of primary suspension	10^6 N/m	1.12×10^6 N/m
Stiffness of secondary suspension	4.3×10^5 N/m	4.3×10^5 N/m
Damping of primary suspension	2×10^4 N s/m	1.2×10^4 N s/m
Damping of secondary suspension	2×10^4 N s/m	2×10^4 N s/m

the reference value, that is

$$\varepsilon = \frac{F_{\max}^{H} - F_{\max}^{NH}}{F_{\max}^{NH}} \times 100 \tag{11}$$

It can be seen that the peak force is overestimated in most of the calculations when the Hertzian model is used. In the studied cases, only the calculations obtained from the rounded flat geometry parameters of Case A give an interval of speeds where the peak force calculated by the non-Hertzian model is slightly higher than that given by the Hertzian model. In most cases, the reduced stiffness of the real contact in the flat vertex (where the impact occurs) gives lower contact force values than with the Hertz model.

The graphs in Figure 11 give examples of the wheel-rail contact forces calculated from both contact models. Results were obtained for a fresh and a rounded flat with the two cases presented in Table 1. Vehicle speeds were selected that gave the greatest difference between the results for the two models: 40 km/h for the fresh flat and 70 km/h for the rounded. It can be observed that for the least dynamically stiff track (Case B) the dynamic response obtained with both contact models was quite similar with the exception of the interval of time where the impact occurs.

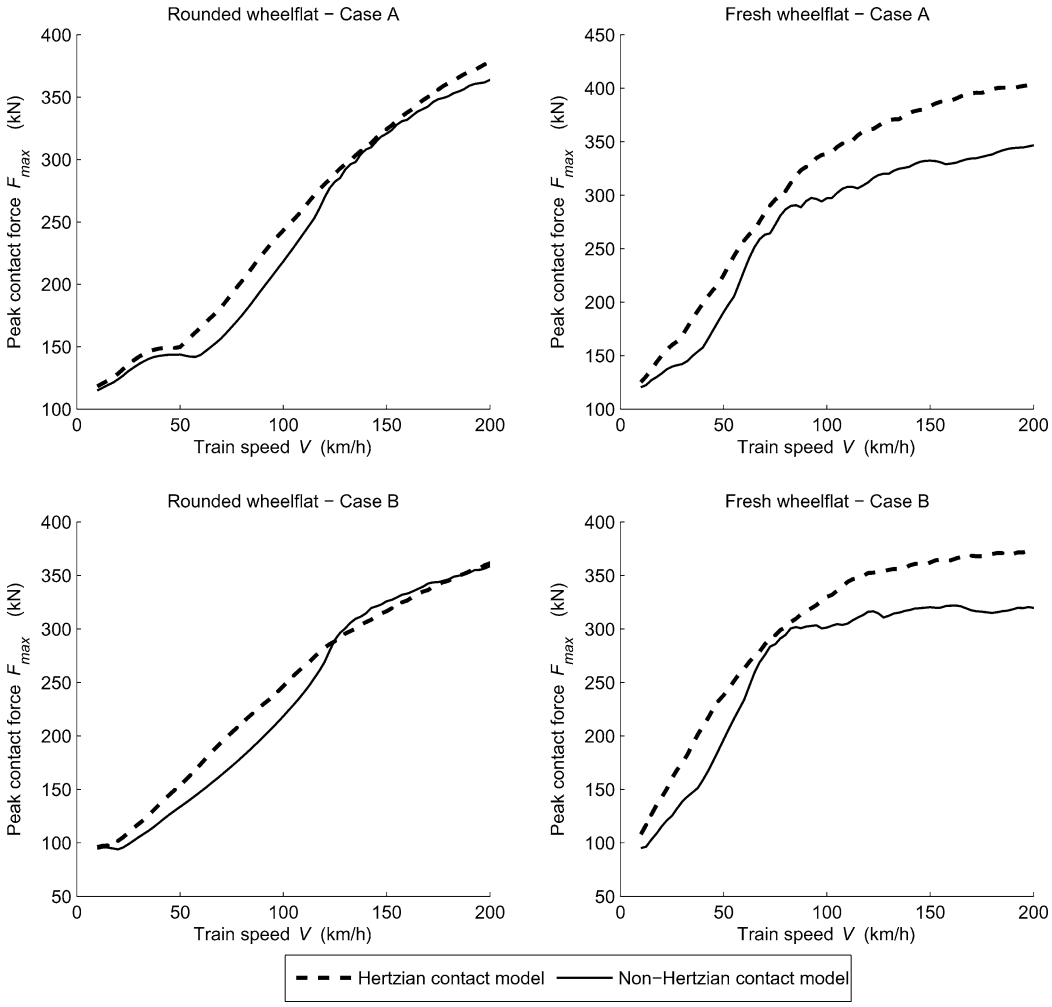

Figure 9. Peak contact force calculated for a set of train speeds. The results have been obtained through the Hertzian and the non-Hertzian contact model.

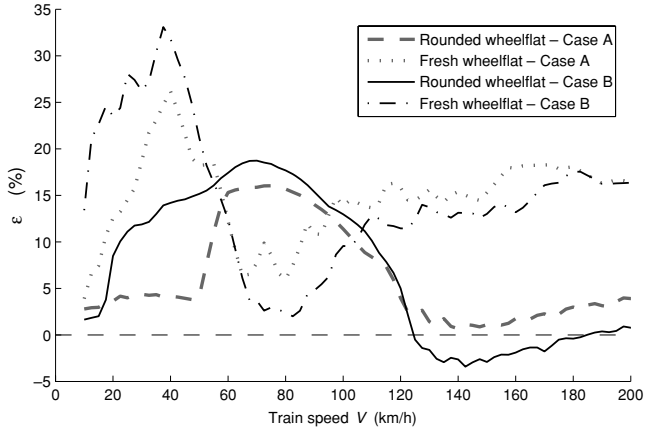

Figure 10. Relative error of the peak contact force value calculated with the Hertzian contact model for fresh and rounded flats (Reference value: peak contact force calculated with the non-Hertzian model).

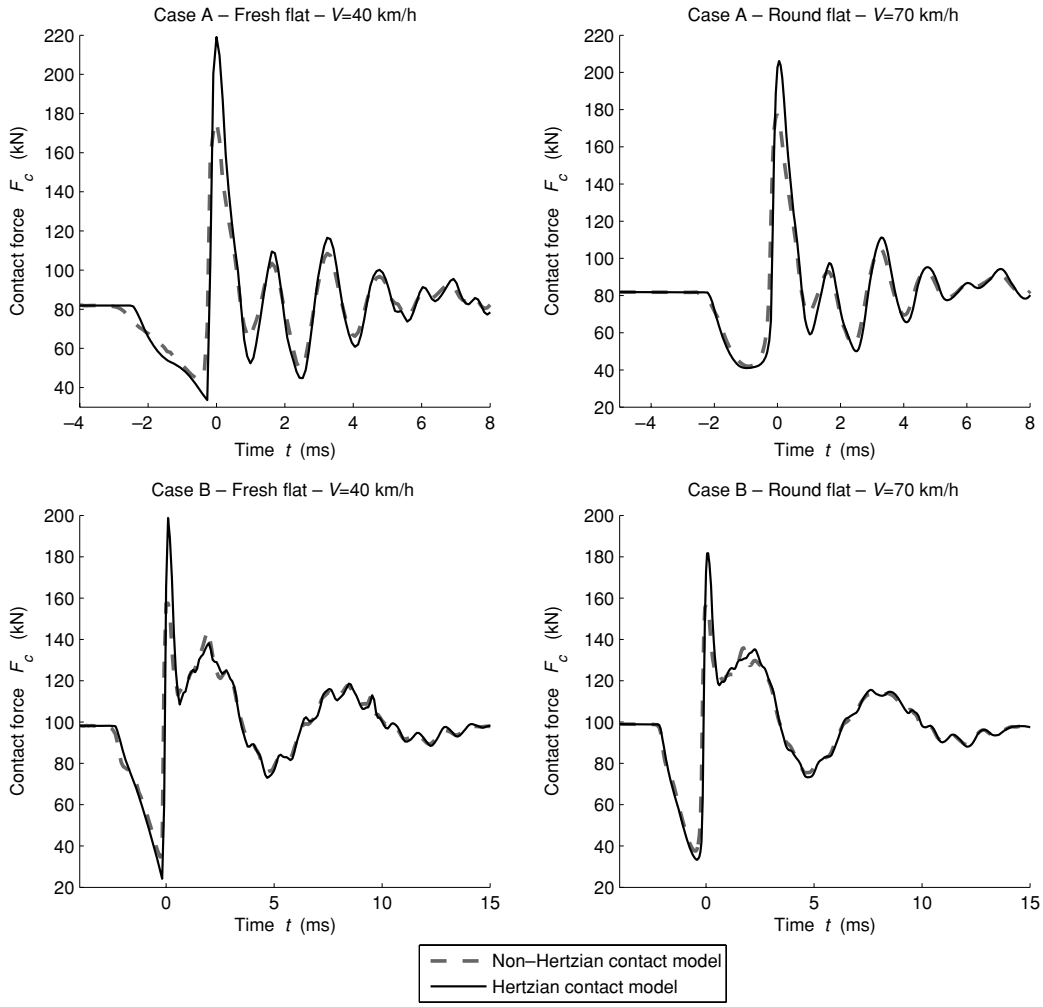

Figure 11. Contact forces caused by a fresh flat and a rounded flat when the vehicle was running at 40 and 70 km/h calculated by Hertzian and non-Hertzian contact models.

7. Conclusions

A methodology developed in a previous work to calculate the dynamic train-track response has been adapted in order to include wheel-rail non-Hertzian contact models. Using this technique, the vibratory response caused by a vehicle affected by a wheelflat was analyzed by both Hertzian and non-Hertzian contact models. From the results obtained it can be observed that the peak value of the force transmitted as calculated by the non-Hertzian model is significantly lower in most of the cases studied. In the simulations performed, a deviation can be observed from the results of the Hertzian model that can exceed 30% of the real peak value. On the other hand, the response outside the moment of impact is not significantly influenced by the contact model, especially when the dynamic stiffness of the track is low. These conclusions could contribute to explain the causes of the deviations detected with regard to the theoretical simulation models and the impact detectors based on the peak value of the contact force.

Acknowledgements

The authors wish to express their gratitude for the support received in the course of this work from the Spanish Ministry of Education and Science through the Research Project TRA2004-01828/TREN and to the Autonomous Government of Valencia for its help through the program Grupos 04/63.

References

1. UIC. *Atlas of Wheel and Rail Defects*. ISBN 2-7461-0818-6. Paris, 2004.
2. Nielsen, J. C. O. and Johansson, A., 'Out-of-round railway wheels – a literature survey', in *Proceedings of the I MECH E Part F Journal of Rail and Rapid Transit*, Vol. **214**(F), 2000, pp. 79–91.
3. Johansson, A. and Nielsen, J. C. O., 'Out-of-round railway wheels-wheel-rail contact forces and track response derived from field tests and numerical simulations', *Proceedings of the I MECH E Part F Journal of Rail and Rapid Transit*, **217**, 2003, 135–146.
4. Nielsen, J. C. O., Ringsberg, J. W., and Baeza, L., 'Influence of railway flat impact on crack growth in rails', *8th International Heavy Haul Conference*. Rio de Janeiro, 2005.
5. Andersson, C., *Modelling and Simulation of Train-track Interaction Including Wear*, Ph.D. Thesis, Department of Applied Mechanics, Chalmers University of Technology, Göteborg, 2003.
6. Wu, T. X. and Thompson, D. J., 'A hybrid model for the noise generation due to railway wheel flats', *Journal of Sound and Vibration* **251**(1), 2002, 115–139.
7. Nielsen, J. B., 'Evolution of rail corrugation predicted with a non-linear wear model', *Journal of Sound and Vibration* **227**(5), 1999, 915–933.
8. Kik, W. and Piotrowski, J., 'A fast, approximate method to calculate normal load at contact between wheel and rail and creep forces during rolling', I. Zobory (ed.), in *Proceedings of the Second Mini Conference on Contact Mechanics and Wear of Rail/Wheel System*, Budapest, 1996.
9. Johnson, K. L., *Contact Mechanics*, Cambridge University Press, 1985, ISBN 0-521-34796-3.
10. Kalker, J. J., *Three-Dimensional Elastic Bodies in Rolling Contact*, Kluwer, Dordrecht, 1990. ISBN 0-7923-0712-7.
11. Baeza, L., Roda, A. and Nielsen, J. C. O., 'Railway vehicle/track interaction analysis using a modal substructuring approach', To be published in *Journal of Sound and Vibration*.
12. Thompson, J. M. T. and Bishop, S. R. (ed.), *Nonlinearity and Chaos in Engineering Dynamics*, Wiley, New York, 1993. ISBN 0-471-94458-0.
13. Tunna, J. M., 'Wheel/rail forces due to wheel irregularities', in *Proceedings of the 9th International Wheelset Congress*, Montreal, paper 6–2, 1988.
14. Hills, D. A. and Nowell, D., *Mechanics of Fretting Fatigue*, Kluwer, Dordrecht, 1994, ISBN 0-7923-2866-3.
15. Love, A. E. H., *A Treatise on the Mathematical Theory of the Elasticity*, Cambrige University Press, Cambridge, 1952.
16. Newton, S. G. and Clark, R. A., 'An investigation into the dynamic effects on the track of wheelflats on railway vehicles', *Proceedings of the Institution of Mechanical Engineers, Part C: Journal of Mechanical Engineering Science* **21**(4), 1979, 287–297.
17. Johansson, A. and Nielsen, J. C. O., 'Out-of-round railway wheels – wheel-rail contact forces and track response derived from field tests and numerical simulations', *Proceedings of the Institution of Mechanical Engineers, Part F: Journal of Rail and Rapid Transit* **217**, 2003, 135–146.